

Multi-Ion Analysis of RBE using the Microdosimetric Kinetic Model

Council of Ionizing Radiation Measurements and Standards (CIRMS)
March 28th, 2017

Michael P. Butkus^{1,2}

Todd S. Palmer²

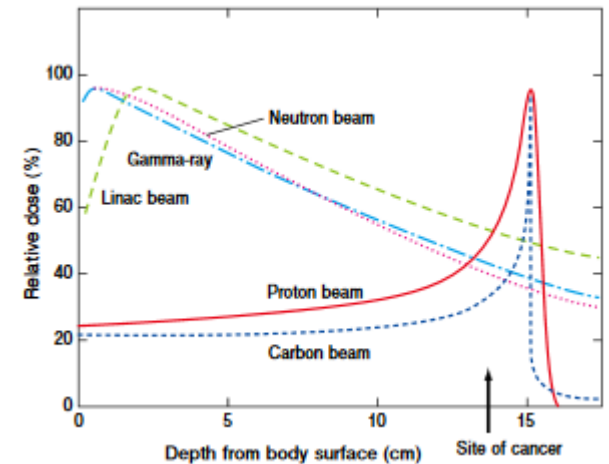
¹Yale School of Medicine: Therapeutic Radiology

²Oregon State University: Dept. of Nuclear Engineering, Health Physics and Medical Physics

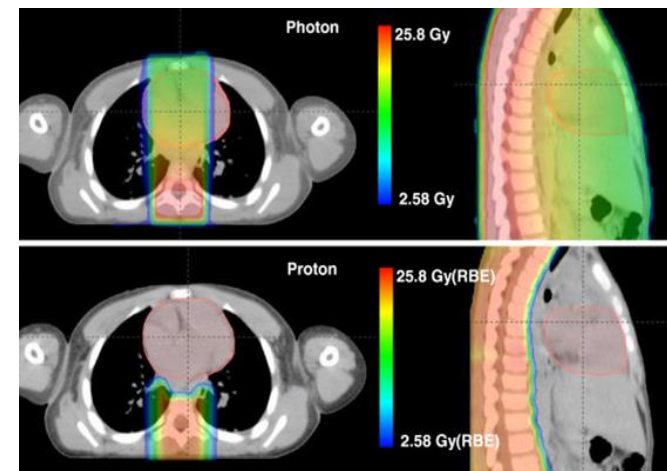


Rationale

- Inverse depth-dose profile of ions make them a highly attractive modality to spare healthy tissues proximal to a lesion.
 - Rapid dose fall-off able to spare critical structures immediately distal to a lesion.
- In theory, higher charged ions provide greater sparing both proximally and distal.
 - In reality, fragmentation of more massive ions limit their utility.
- Compared to equivalent physical doses, ions have demonstrated enhanced cell killing rates over photons.
 - The increase in relative biological effectiveness (RBE) is inversely related to penetration depth, amplifying the advantages of ions.



Furusawa. Rad Sci. (2007)



Zhang et. al. Rad Onc (2013)

Historical Usage

- 1929: Lawrence patents first working cyclotron
- 1938: “Successful” neutron therapy conducted
- 1946: Wilson publish “Radiological use of fast protons”¹
- 1954: Canine pituitary treatments performed at Berkeley with protons
- 1954: Treatments begin on human pituitary gland
 - Ease of localization prior to CT
- 1974: BEVELEC: Treatments using various ions (^4He , ^{20}Ne , ^{40}Ar)
 - MGH, Uppsala, others begin trials
- 1990: Loma Linda opens first dedicated clinical proton beam
- 1994/1997: HIMAC and GSI begin ^{12}C treatments
- Last Decade: Massive increase in proton facilities, large relative increase of ^{12}C clinics.

Current Status

- PTCOG 2016 Report²:
 - Protons: 63 clinics, 150+ treatment rooms, 130,000+ patients
 - ¹²C: 8 clinics, 23 treatment rooms, 19,000 patients
 - Historically (1957-1992) 2054 patients treated with ⁴He and 433 treated with other ions.
 - Advances in accelerator design have created more economical and standardized delivery platforms.
 - Pencil beam scanning in lieu of passive scattering have reduced neutron contamination and fragmentation shortcomings (still a major concern though!)
 - Improvements in imaging allow for more conformal treatments.

Shortcomings

- Quantitative uncertainties in cellular responses
 - Lack of agreement between centers on calculation of RBE
- Majority of expertise and clinical outcomes acquired with passively spread beams
 - And only with protons and ^{12}C beams
- Less robust than modern photon treatments

- *US-DOE/NIH/NCI/HHS “Workshop on Ion Beam Therapy” (2013)*³
 - Primary Charge
 - Reduce uncertainties in biological effect
 - Secondary Charges
 - Investigate potential of novel ions
 - Investigate effect of small diameter beams

Difference between Proton and Light Ion Therapy

Major differences exist between protons and other light ions

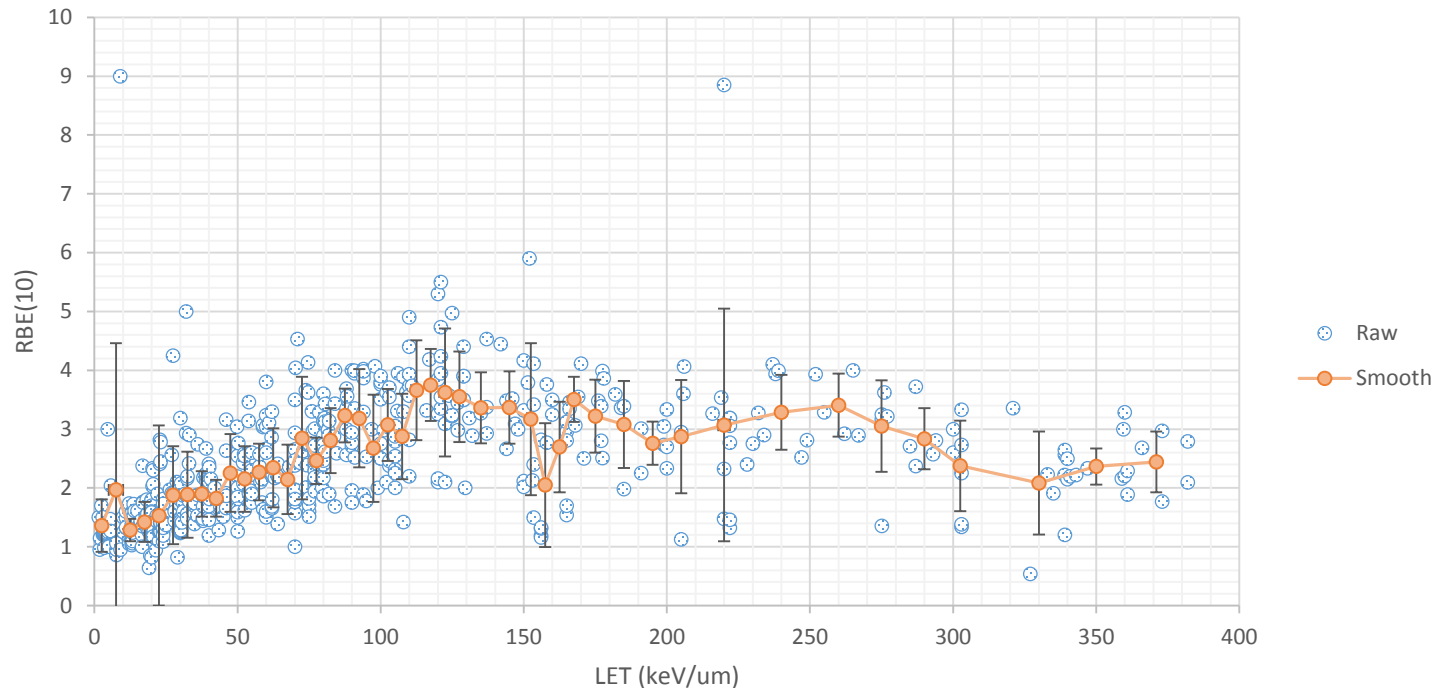
	Protons	Light Ion
Atomic Mass (amu)	1	2-20
Fragmentation	No	Yes
Nuclear Reactions	Yes	Yes
Range Straggling	Yes	Reduces with Z^2
Lateral Deflection	Large	Reduces with particle mass
Lateral Penumbra	Small	Increases with particle energy
Bragg Prominence	No contamination	Increases with Z^2
LET	Low	High
RBE	Clinically assumed 1.1	~1-5 (large uncertainties)
RBE variance	Assumed Constant	Known to fluctuate with energy
Major Clinical Advantage	Dose Conformity	Dose Conformity and Elevated RBE .
Major Clinical disadvantage	Low RBE, Cost, Expertise	Fragmentation, Cost, Expertise

Although many similarities are shared between proton and light ion treatments, this presentation will primarily focus on light ion therapy which have a greater biological advantage than protons.

Linear Energy Transferred (LET) and RBE

- Ion RBE is commonly reported as a function of linear energy transferred (LET).
 - RBE initially increases with LET (as an ion loses kinetic energy)
 - Maximum occurs around $\sim 100\text{-}150$ keV/ μm
 - Then decreases due to “overkill” effect
- However, LET is an averaged value taken over ranges greater than that of cellular DNA.
 - Ignores stochastic nature of energy deposition at cellular levels
 - Does not account for spatial distribution of delta rays
- May be an inappropriate metric to evaluate RBE by...
 - Data is very spread.
 - Different particles with equivalent LET vary in cell killing efficiency
 - Different cell types respond to similar radiation differently

LET to define RBE?

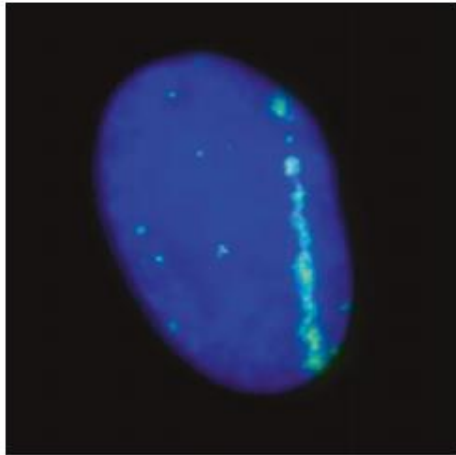


- Compendium of reported RBE vs. LET values from 70 papers (650+ values)
- Qualitative trend can be seen, but data is very spread.
- Lack of reproducibility between studies and standardization of measurements.
- Could RBE be dependent on more than LET?

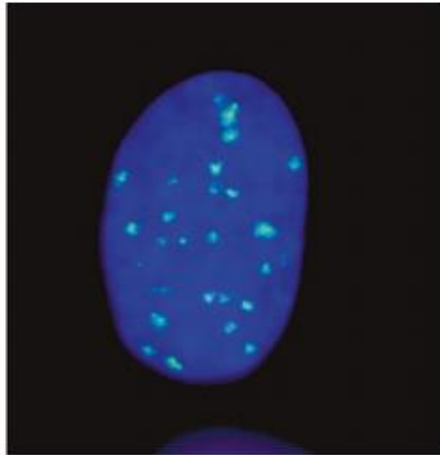
Note: Not all reviewed data reported errors, or reported similar style errors so raw data (blue dots) reported as absolute. (Sorry NIST ☹)

RBE dependence on ion charge

Ions



Photons

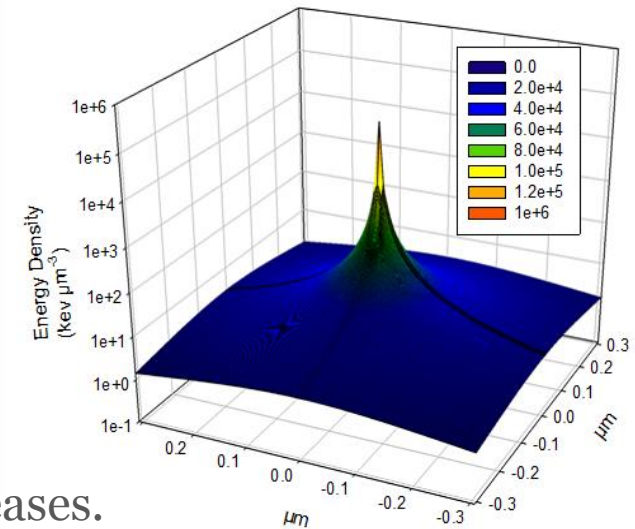


Furusawa (2014)

Chatterjee⁴ Ionization density radii

$$r_{core} = 0.0116\beta$$

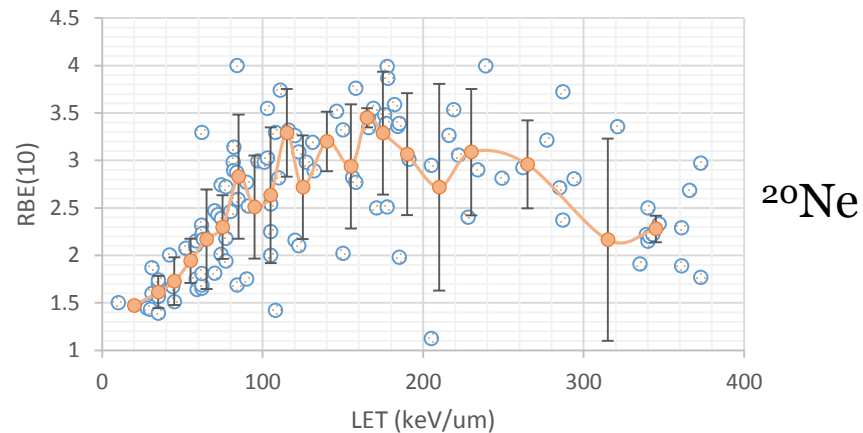
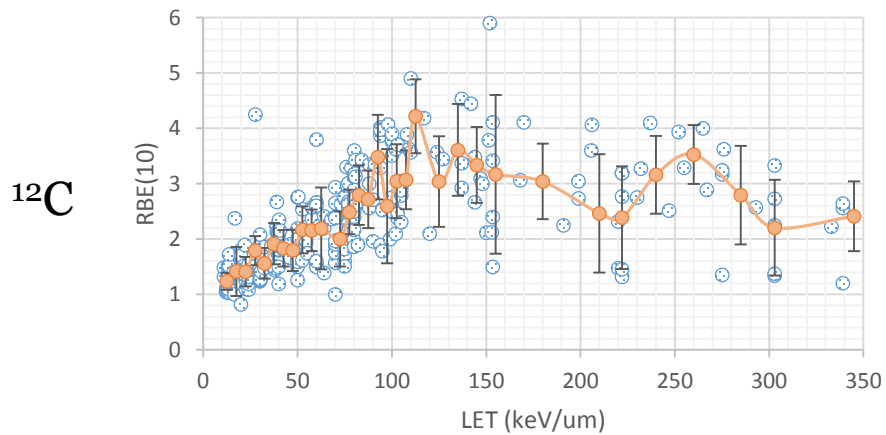
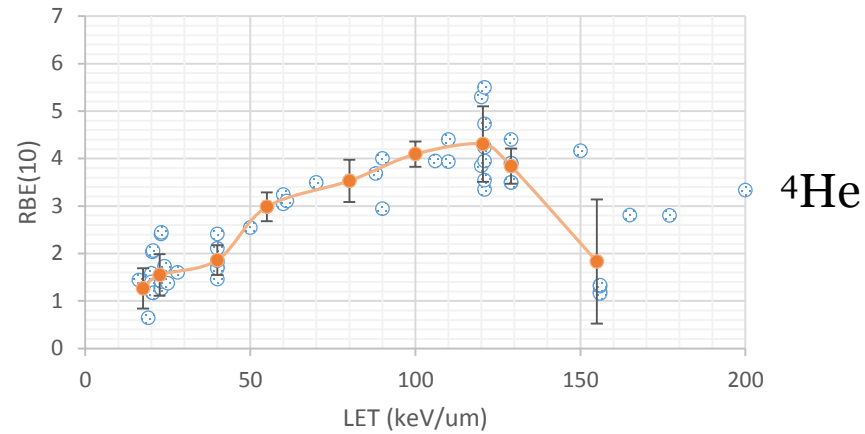
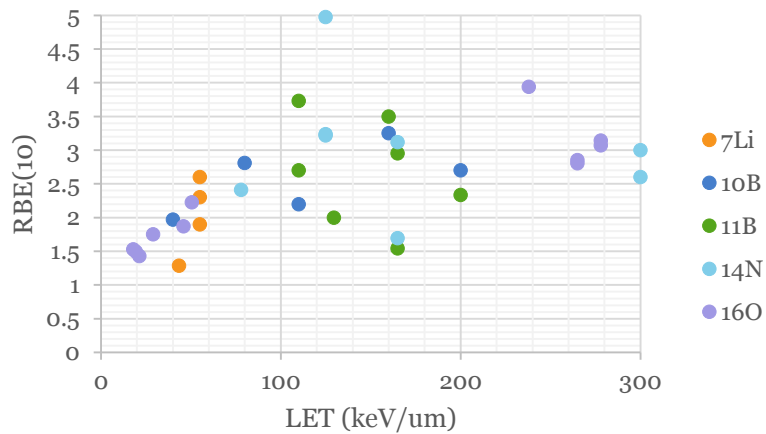
$$r_{penumbra} = 0.768E - 1.925\sqrt{E} + 1.257$$



296 MeV/amu, ²⁰Ne, in tissue

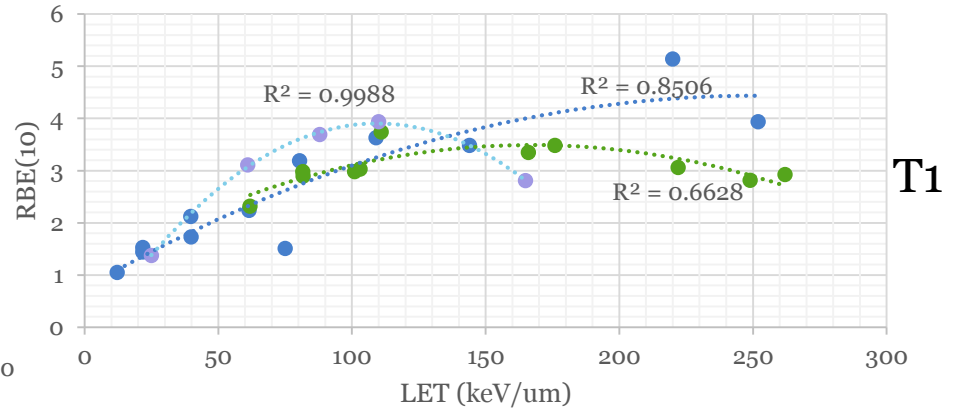
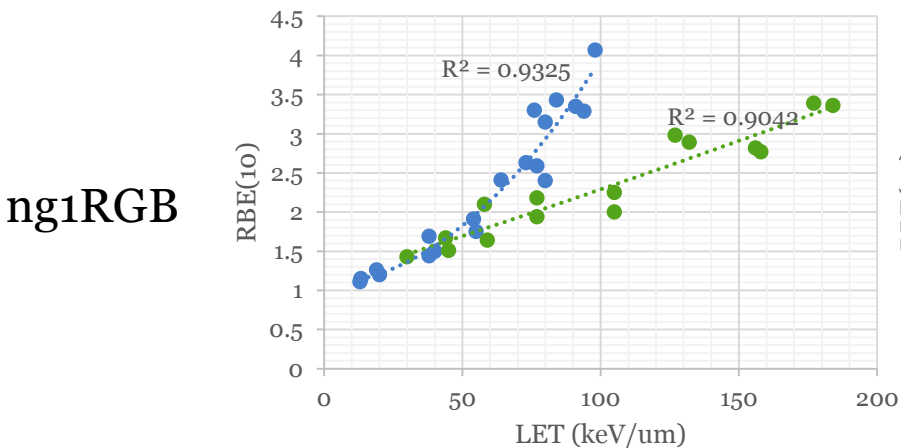
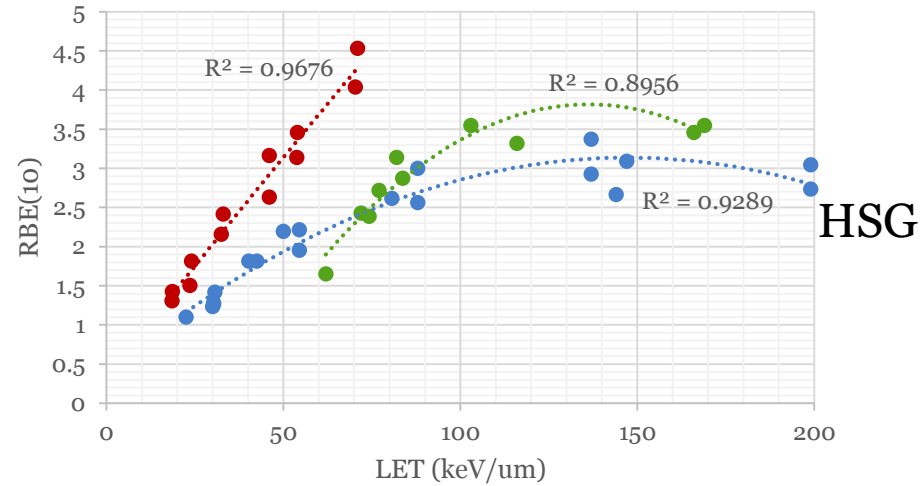
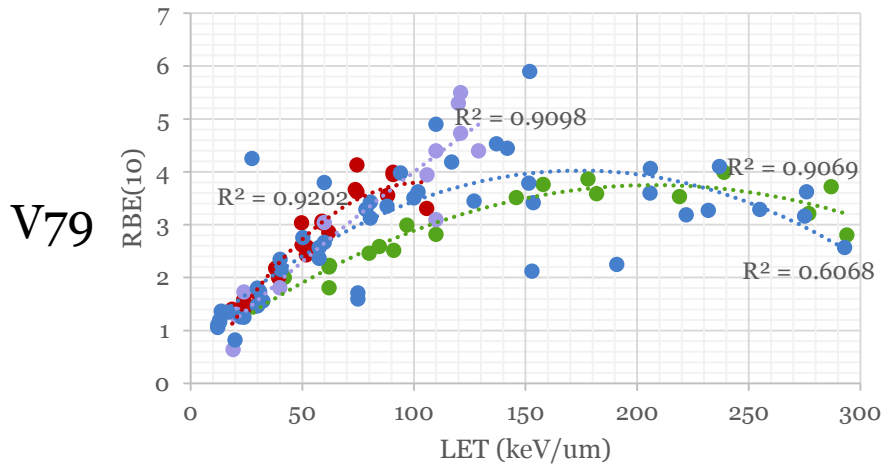
- As a particle slows down its ionization density increases.
- Heavier ions of the same velocity have greater energy, and thus larger penumbras
- Particles of the same LET have dissimilar radial profiles

RBE dependence on ion charge



Note: Not all reviewed data reported errors, or reported similar style errors so raw data reported as absolute. (Sorry NIST ☹)

RBE dependence on ion charge and cell type

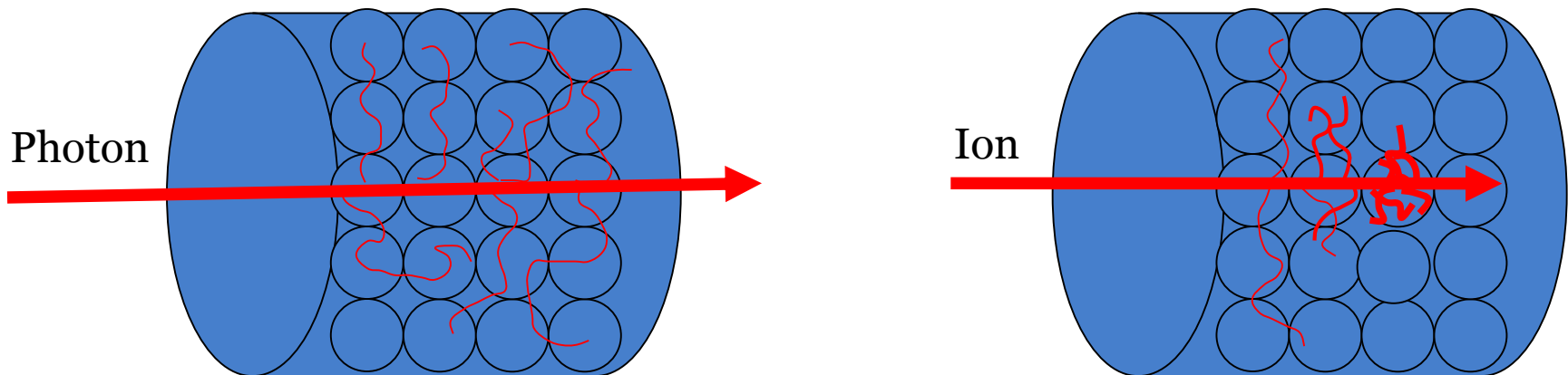


^3He (red), ^4He (purple), ^{12}C (blue), ^{20}Ne (green)

Note: Not all reviewed data reported errors, or reported similar style errors so raw data reported as absolute. Best fit lines are for 2nd order polynomials

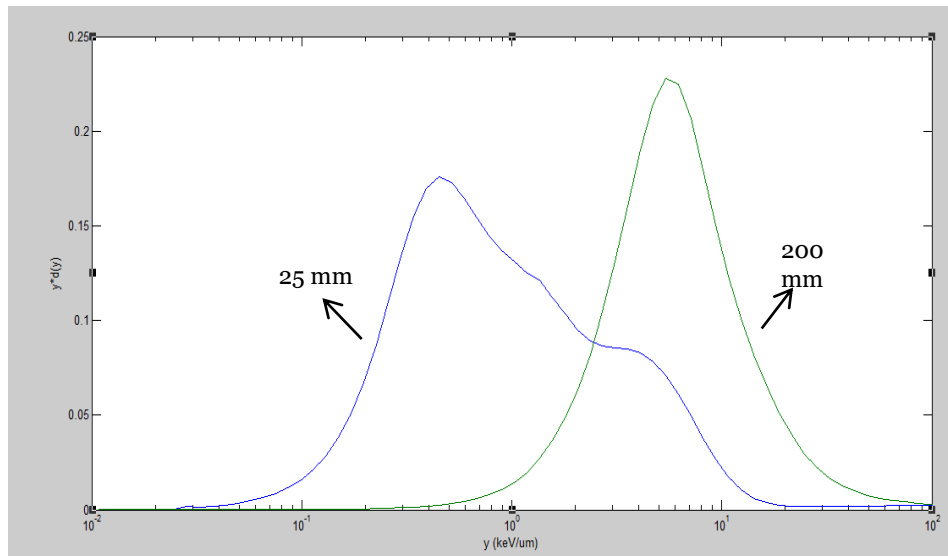
What can be used other than LET?

- An alternative from LET may be needed that also accounts for particle type, cell type, and spatial distributions.
- DNA is target for cell death, so parameter additionally has to account for stochastic nature of deposition on micrometer scale.
- Microdosimetry: A higher fidelity analysis of the stochastic dose deposition that is averaged out on the scale of conventional dosimetry



Microdosimetric Quantities

- Specific Energy, analogous to macroscopic absorbed dose.
 - $z = \epsilon/m$ (total energy absorbed in a microscopic site by mass)
- Lineal Energy, analogous to LET
 - $y = \epsilon/\bar{l}$ (energy absorbed from correlated event by average chord length of microscopic site)
- Since z and y are stochastic, best to represent them by their probability distributions, $f(z)$ and $f(y)$.



LET of particles only vary by $\sim 0.5 \text{ keV/um}$. However, less energetic beam deposits dose from less, but more energetic events.

Expectation Values

$$\bar{z}_D = \int_0^{\infty} z d_1(z) dz$$

$$\bar{y}_D = \int_0^{\infty} y d(y) dy$$

Microdosimetric Kinetic Model (MKM)

- Based upon cellular theories of:
 - Dual Radiation Action
 - Repair-Misrepair
 - Lethal-Potentially Lethal
- Cellular volume comprised of hundreds of “domains” which act as relevant energy transfer points.
- One of three models currently to determine clinical RBE of light ions.

MKM Assumptions

- I. Damage mechanisms are the same for all radiation types
- II. RBE differences are solely due to differences in spatial and temporal distribution of deposition events
- III. Deposition events can cause lethal (λ_d) or sub-lethal damage (k_d). Sub-lethal damage can:
 - i. Spontaneously transformation into a lethal lesion by a first order process, a ,
 - ii. Interact with other sub-lethal lesions in the same domain to create a lethal lesion by a second order process, b ,
 - iii. Spontaneous repair by a first order process, c ,
 - iv. Remain unchanged for a time, t_r , after which time, it becomes a lethal lesion.
- IV. Domain is considered dead if in contains a single lethal lesion
- V. Cell is considered dead if a domain in its nucleus is considered dead
- VI. Yield of lethal and sub-lethal lesions is proportional to the specific energy, z_d , or lineal energy, y_d , deposited in the domain

Cell Survival with MKM (Modified for Overkill effect)

- Cell survival probability (S) can be modeled as:

$$S = \exp \left\{ - \left[\alpha_0 + \beta * \frac{y_0^2}{\rho \pi r_d^2} \frac{\int [1 - \exp[-(y^2/y_0^2)] f(y) dy]}{\int y f(y) dy} \right] * D - \beta D^2 \right\}$$

- α_0 = Initial slope of cell survival curve for LET=0
- β = constant in MKM
- y_0 = saturation parameter

$$y_0 = \frac{l_d}{m_d} \frac{\rho_d \pi r_d r_n^2}{\sqrt{\beta_0 (r_d^2 - r_n^2)}}$$

- Reduces to a linear quadratic form:

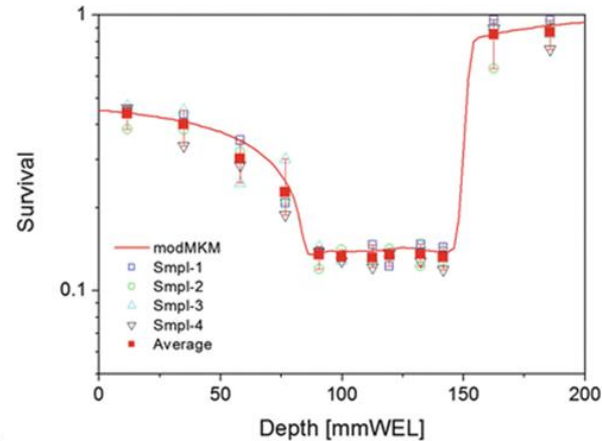
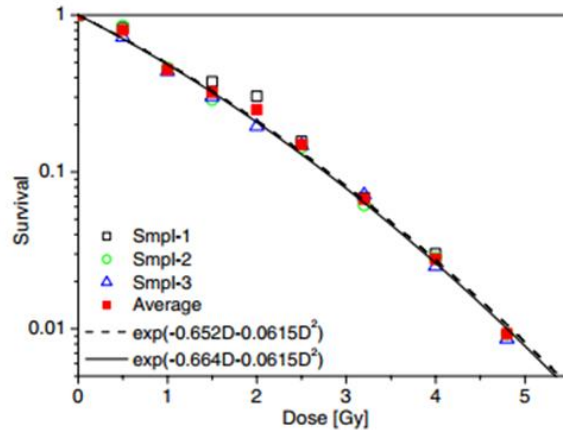
$$\ln(S(D)) = -\alpha_c D - \beta_0 D^2$$

- For photons:

$$\ln(S(D)) = -\alpha_X D - \beta_0 D^2$$

y^*

Results of MKM



Relationship between measured cell survival and theoretical prediction from the modified microdosimetric kinetic model for HSG tumor cells irradiated with 290 MeV/amu ^{12}C ions. (Inaniwa, T (2010))

Strong agreements between the modified MKM and measured cell survival has lead NIRS to begin implementation of the model into their clinical treatment planning system.

Experimental Purpose

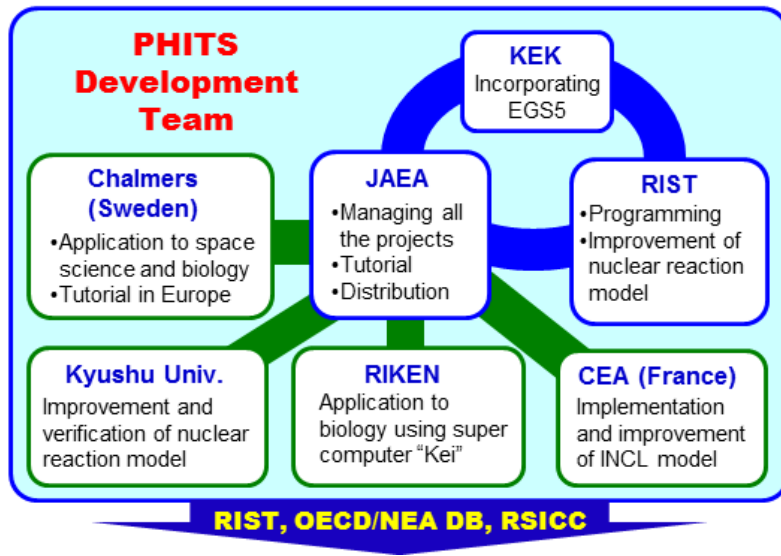
- RBE for ions can be solved from the single parameters y^* or Z_D^*
 - As long as cellular parameters are known.
- We will calculate y^* from lineal energy probability distribution functions and solve RBE for different ionic species
 - At clinically relevant depths
 - Using a small diameter pencil beam to simulate a scanned treatment beam
- RBE values will be multiplied by macroscopic dose to determine optimal ion species for each penetration depth.

Methodology

- Must obtain probability densities to establish y^*
 - Unfeasible to measure these in body, must use simulation code
- Microscopic track structure codes capable of simulating probability densities
 - Most function only for single monoenergetic particles
 - In body, fragmentation creates multiple ion, polyenergetic spectrum
- Macroscopic codes can simulate diverse spectrum
- Computational limits makes coupling of macro and microscopic codes infeasible.
- Particle Heavy Ion Transport System (PHITS)⁵ capable of applying analytical microscopic function to macroscopic simulation to overcome computational time limits.

PHITS-Macroscopic Simulation

- General purpose Monte Carlo code capable of transporting all particles types to energies of 100 GeV/amu



	Neutron	Proton, Pion (other hadrons)	Nucleus	Muon	Electron /Positron	Photon
High Energy ↑	200 GeV	Intra-nuclear cascade (JAM) + Evaporation (GEM)	100 GeV/n Quantum Molecular Dynamics (JQMD) + Evaporation (GEM)			100 GeV Atomic Data Library JENDL-4.0 / EPDL97
	3.0 GeV	Intra-nuclear cascade (INCL4.6) + Evaporation (GEM)	10 MeV/n Evaporation (GEM)		100 MeV Atomic Data Library (EEDL/ITS3.0/EPDL97)	140 MeV Photo-Nuclear
Low Energy ↓	20 MeV Nuclear Data Library (JENDL-4.0)	1 MeV 1 keV	10 MeV/n Ionization SPAR or ATIMA		1 keV	1 keV
	10 ⁻⁵ eV					

PHITS (2017)

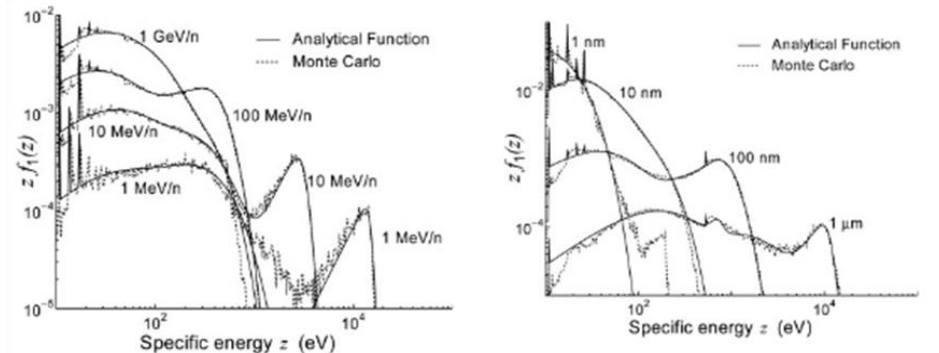
PHITS-Microscopic Calculation

- Probability densities calculated around multiple ions of varying energy using microscopic code TRACEL.
- Creation of function to reproduce TRACEL results.
- Implementation of function into macroscopic code
- Event generator mode
 - Ions transported to 1E^{-10} MeV to get appropriate charge, energy, LET of secondary particles

$$\epsilon f_1(\epsilon, \varphi_s, Z, E, L) = \frac{A(\varphi_s, Z, E)\epsilon^2}{\exp\{B(\varphi_s, Z, E)[\epsilon - C(\varphi_s, Z, E)L\varphi_s]\}} + \sum_{k=1}^2 \frac{\mu_k(\varphi_s, Z, E)\epsilon}{[j_k(\varphi_s, Z, E) - 1]} \left[\frac{j_k(\varphi_s, Z, E) - 1}{j_k(\varphi_s, Z, E)} \right] \frac{\epsilon}{\omega} + \sum_{i=1}^6 P_i(\varphi_s, Z, E)\delta(\epsilon_{pi}) + \frac{P_7(\varphi_s, Z, E)}{\sqrt{2\pi}\Gamma} \exp\left[-\frac{(\epsilon - \epsilon_{p7})^2}{2\Gamma^2}\right]$$

Function of:

- Deposition energy
- Domain diameter
- Particle charge
- Particle energy
- Unrestricted LET

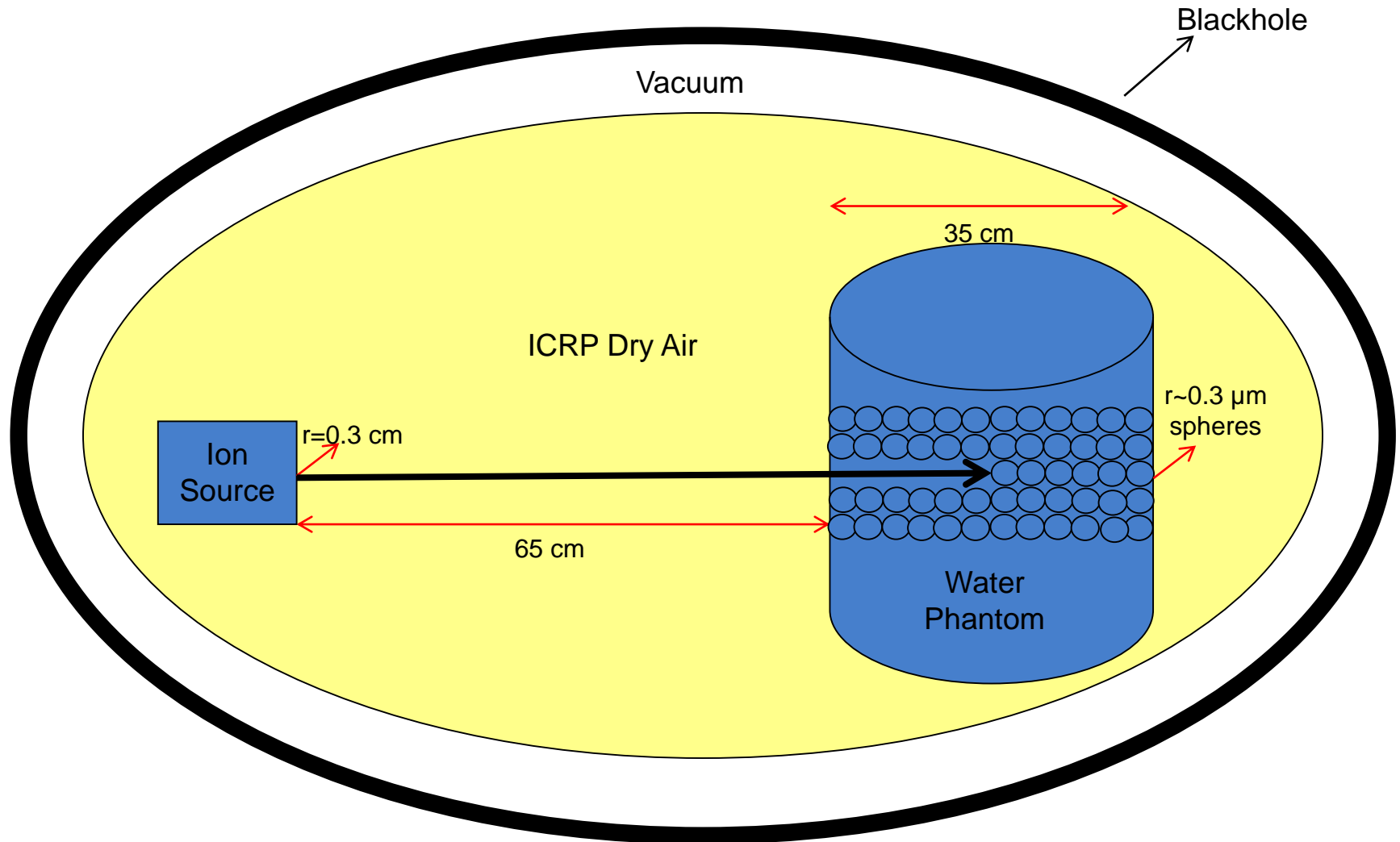


Sato (2006)

Execution

- PHITS version 2.62 (03/20/2015)
- Large scale simulations ran on Oregon State High Performance Computing Cluster in shared memory mode
 - Between 80 and 200 processors per simulation
 - Roughly 960-4300 computational hours per simulation
- 9,000-31,500 macroscopic dose data points collected per simulation
- 1,440,000-5,400,000 microscopic lineal energy data points collected per simulation
- All data processing/analysis done in MATLAB R2014a (Version 8.3.0.532. Released 2/11/2014).

Setup



Ions Simulated

Bragg Peak Depth (cm)	5.0	10.0	15.0	20.0	25.0	30.0	Particles Tracked
Ion	MeV/amu						
¹ H	80.0	117.0	147.0	173.5	197.0	219.25	All, ¹ H
⁴ He	79.5	117.0	147.0	173.5	197.25	219.5	All, ⁴ He, ³ He, ² H, ¹ H
⁷ Li	92.0	135.0	170.0	200.5	228.5	254.5	All, ⁷ Li, ⁶ Li, ⁴ He, ² H, ¹ H
¹¹ B	125.5	186.5	236.5	281.5	321.0	358.75	All, ¹¹ B, ¹⁰ B, ⁴ He, ² H, ¹ H
¹² C	148.5	220.0	279.5	332.5	380.5	426.5	All, ¹² C, ¹¹ C, ⁴ He, ¹ H
¹⁴ N	160.5	240.5	306.0	364.5	419.0	470.0	All, ¹⁴ N, ¹³ N, ¹² C, ⁴ He, ¹ H
¹⁶ O	175.0	260.5	331.75	396.0	455.5	512.0	All, ¹⁶ O, ¹⁵ O, ¹² C, ⁴ He, ¹ H
²⁰ Ne	197.5	297.5	380.5	455.5	525.5	592.0	All, ²⁰ Ne, ¹⁹ Ne, ¹² C, ⁴ He, ¹ H

- 1 MeV/amu uniform energy spread
- 400,000,000 protons for each depth (400 batches of 1,000,000 particles)
- 9,000,000 light ions for each depth (180,000 batches of 50 particles)
- Batch standard deviations of:
 - ~0.01-2% for “All” and primary particle tracking
 - ~0.5-7.0% for secondary particle tracking

Cells Types Simulated

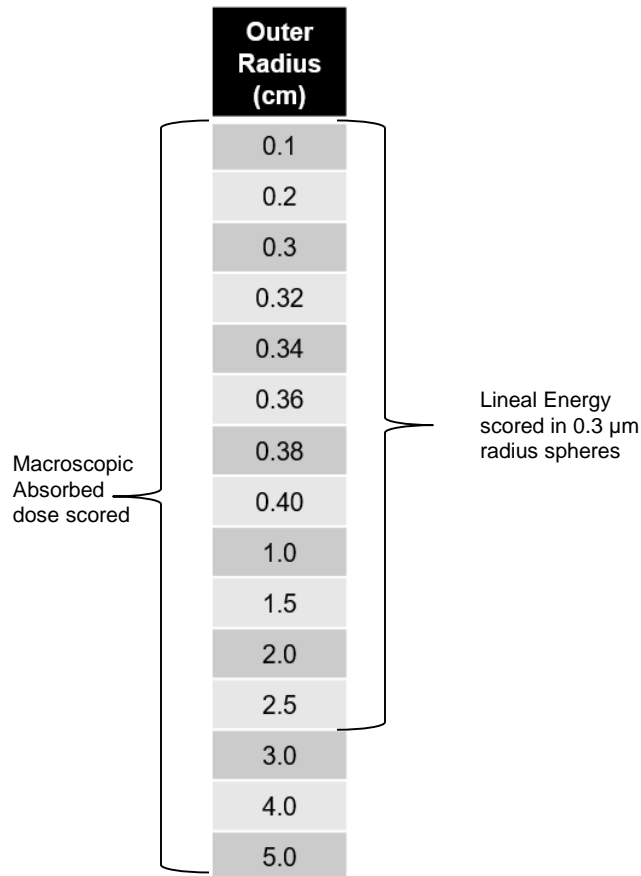
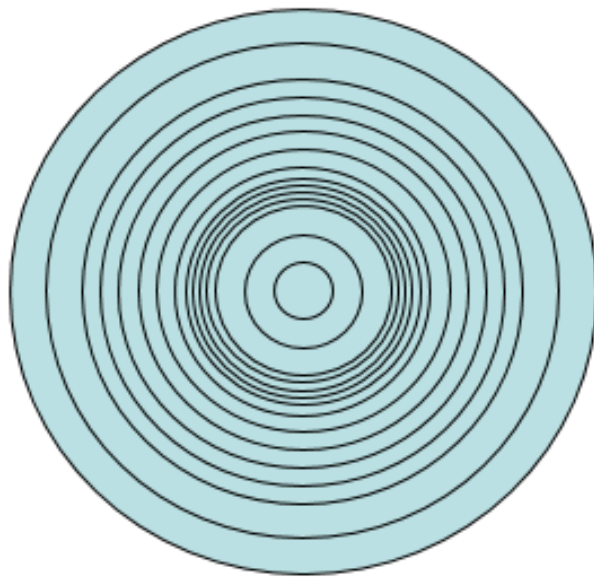
- Human Submandibular (Salivary) Glands
 - Two different sets of parameters reported
 - Used for many ion experiments due to historical experience with high LET neutron head and neck irradiations
- Chinese Hamster V79 lung cells
 - Most commonly used cell for radiobiology experiments
- Normal Human Skin Fibroblast cells (NB1RGB)
 - Non-cancerous cell
- Normal Human T-1 kidney cells.
 - High-LET radiosensitivity

	NB1RGB	V79	T1	HSG-1	HSG-2
Domain (μm)	0.212	0.232	0.326	0.3	0.282
$R_n(\mu\text{m})$	5.44	4.14	4.08	4.2	4.19
$y_0(\text{keV}/\mu\text{m})$	134.4	133.1	107.5	108	93.4
$\alpha_0(\text{Gy}^{-1})$	0.424	0.105	-0.078	0.0777	0.155
$\alpha_x(\text{Gy}^{-1})$	0.559	0.184	0.031	0.192	0.313
$\beta_0(\text{Gy}^{-2})$	0.0283	0.02	0.0585	0.05	0.0615

$\rho=1.0 \text{ g/cm}^3$
for all cells

Scoring

Radial Profile



Absorbed doses and lineal energy scored transversely every millimeter from phantom entrance to Bragg Peak + 5 cm.

Additionally scored radially as shown

Lineal energy bins logarithmically distributed from 0.01 to 10000 keV/ μm . 200 total bins.

RBE Calculation

- RBE evaluated at 10% survival rate,
- Compared to 6MV photon irradiation
- Instantaneous irradiation
- From $f(y)$ data, survival fraction calculated as:

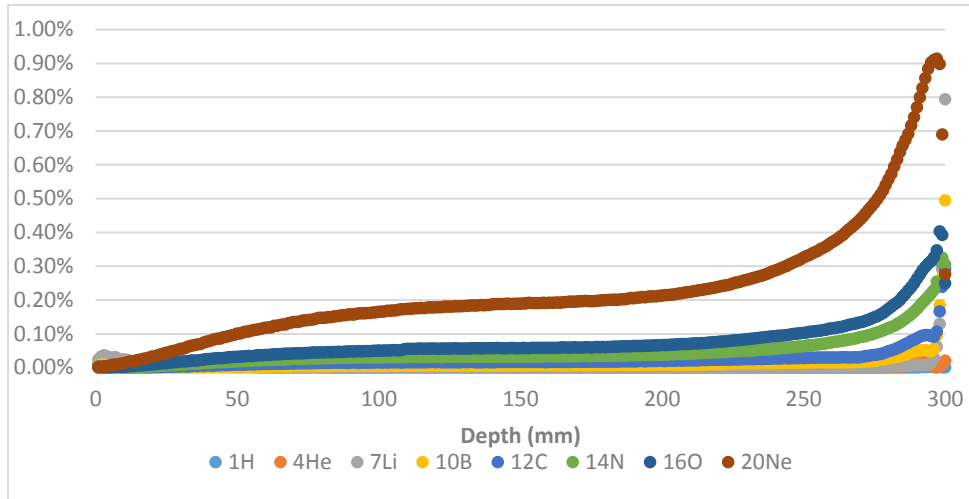
$$S = \exp \left\{ - \left[\alpha_0 + \beta * \frac{y_0^2}{\rho \pi r_d^2} \frac{\int [1 - \exp[-(y^2/y_0^2)] f(y) dy]}{\int y f(y) dy} \right] * D - \beta D^2 \right\}$$

α_c

- And then compared to measured photon values by:

$$RBE = \frac{D_{ref}}{-\alpha_c + \sqrt{\alpha_c^2 - 4\beta \log(S)} / 2\beta}$$

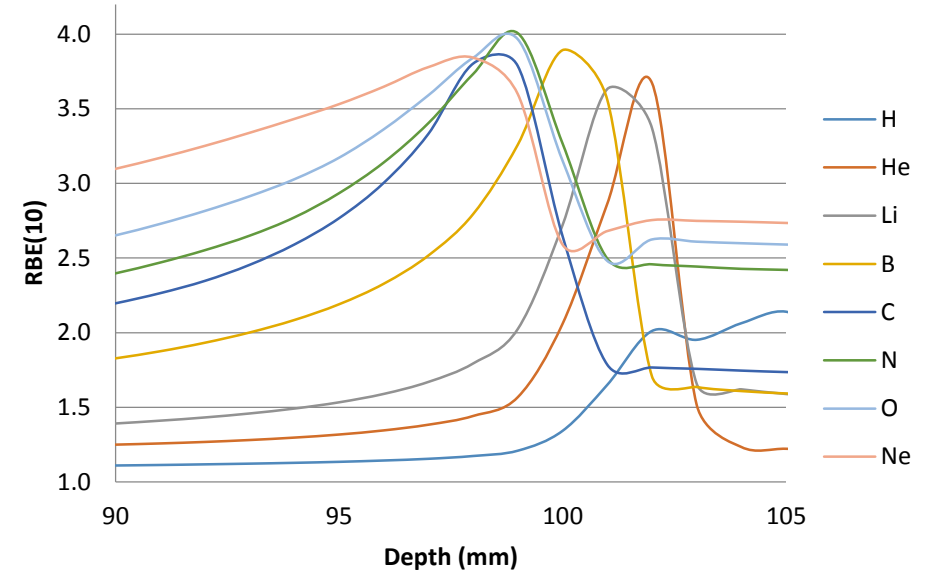
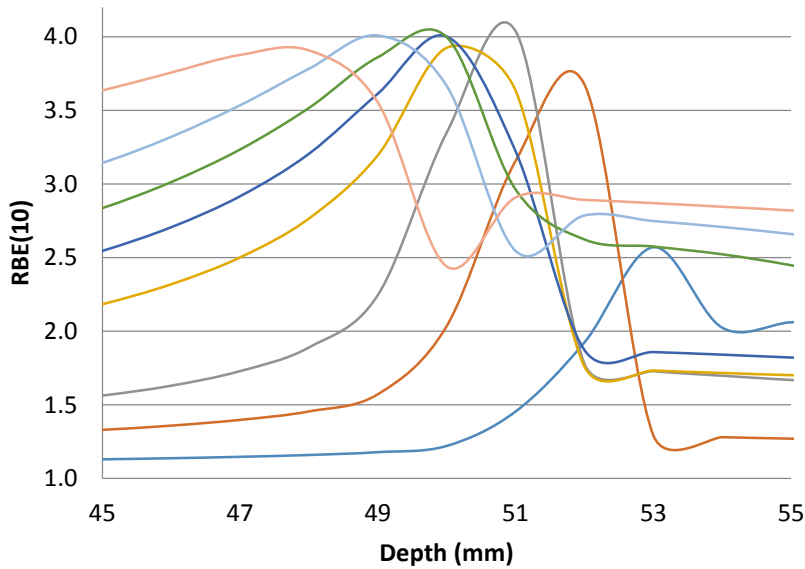
Results: Radial Variance



- Large fluctuations in RBE(10) seen radially from CAX.
- Largest fluctuations seen with heavier ions which displayed minimal deflection.
- However, while biological dose was above 1% CAX dose, maximum variance between CAX RBE(10) and dose weighted RBE(10) was less than 1% at all proximal depths for all ions.
 - Caveat: Distal to the Bragg peak variance could increase to ~5%, but at extremely low dose regions.
- Historical measurements that neglected radial RBE variance will not exhibit large errors due to radial fluctuations.
- The transverse RBE will be described by only the radially dose weighted RBE(10) for the rest of results.

Bragg Peak(mm)	Maximum Dose-Weighted Variance					
	50	100	150	200	250	300
He	0.008%	0.003%	0.032%	0.022%	0.034%	0.029%
Li	0.051%	0.211%	0.360%	0.215%	0.735%	0.794%
B	0.158%	0.185%	0.187%	0.358%	0.428%	0.494%
C	0.214%	0.236%	0.201%	0.189%	0.308%	0.291%
N	0.282%	0.329%	0.300%	0.297%	0.296%	0.325%
O	0.359%	0.449%	0.426%	0.399%	0.410%	0.402%
Ne	0.465%	0.726%	0.683%	0.633%	0.632%	0.914%

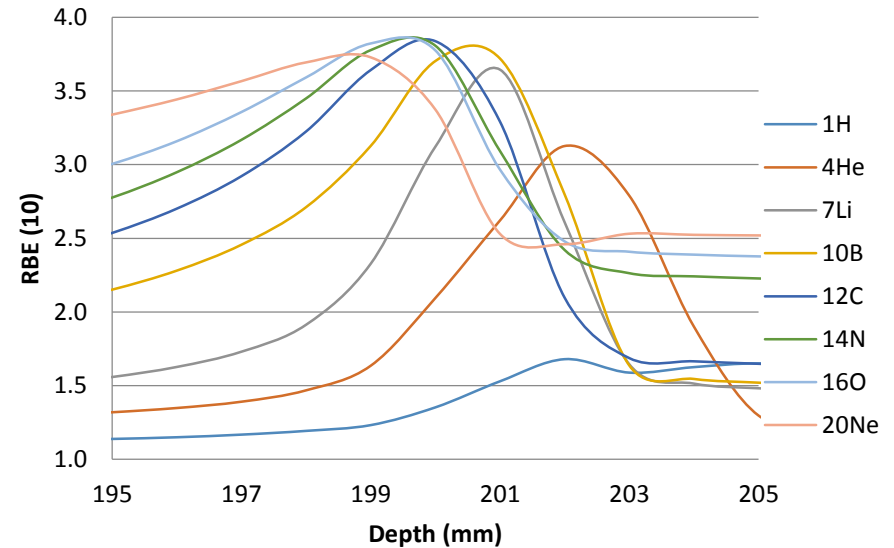
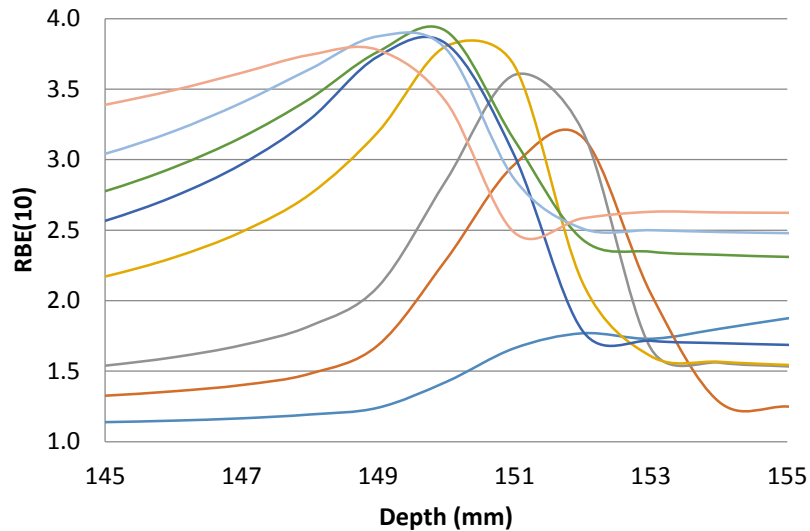
Transverse RBE: 50 and 100mm depth beams



	RBE(10)			Relative Increase From Emtrance			
	Entrance	Bragg	Max	Bragg	σ	Max	σ
He	1.17	2.04	3.68	1.74	0.10	3.14	0.26
Li	1.20	3.35	4.04	2.78	0.07	3.35	0.19
B	1.39	3.93	3.93	2.83	0.13		
C	1.54	4.00	4.00	2.60	0.18		
N	1.69	4.00	4.00	2.37	0.20		
O	1.84	3.67	4.01	1.99	0.23	2.18	0.40
Ne	2.21	2.44	3.91	1.10	0.15	1.77	0.16

	RBE(10)			Relative Increase From Emtrance			
	Entrance	Bragg	Max	Bragg	σ	Max	σ
He	1.13	2.06	3.67	1.82	0.05	3.26	0.11
Li	1.16	2.72	3.63	2.34	0.08	3.12	0.10
B	1.29	3.89	3.89	3.03	0.14		
C	1.40	3.79	3.80	2.71	0.07	2.72	0.09
N	1.49	4.01	4.01	2.68	0.17		
O	1.61	3.15	3.97	1.96	0.25	2.47	0.19
Ne	1.87	2.59	3.84	1.38	0.19	2.05	0.17

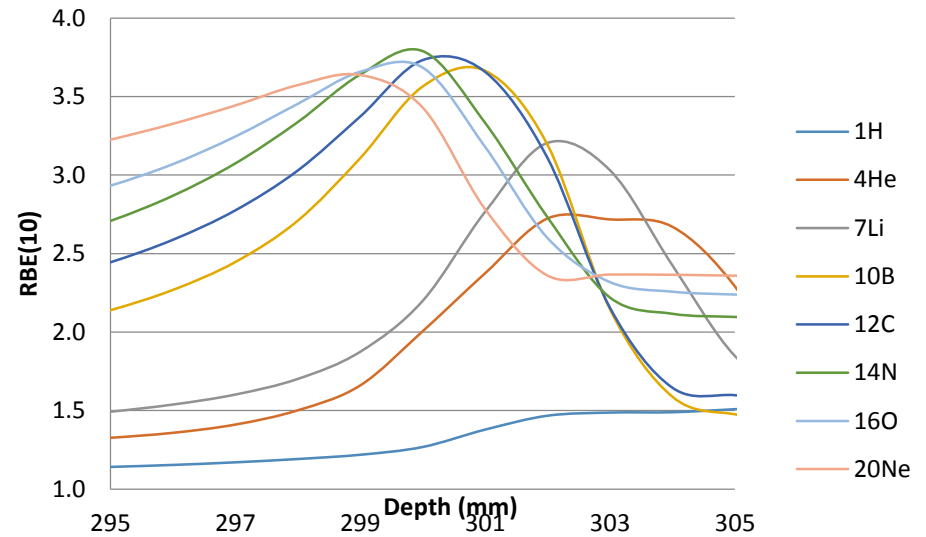
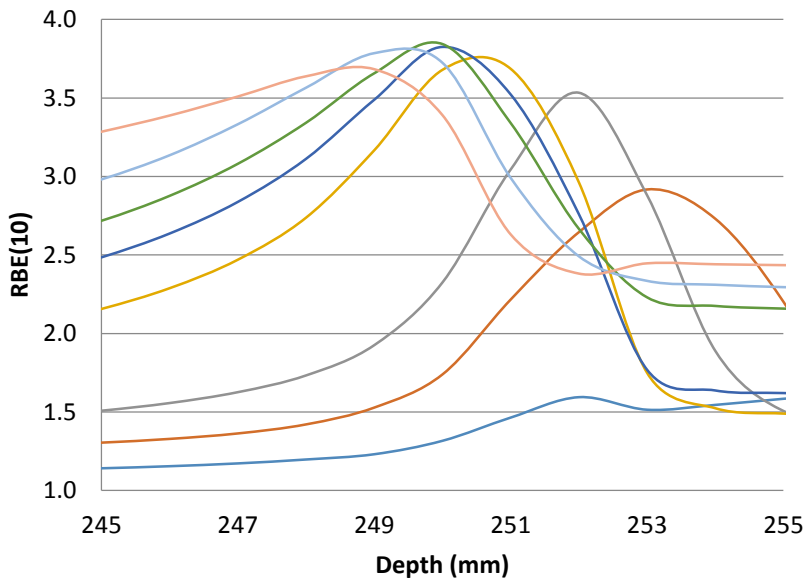
Transverse RBE: 150 and 200mm depth beams



	RBE(10)			Relative Increase From Emtrance			
	Entrance	Bragg	Max	Bragg	σ	Max	σ
He	1.11	2.29	3.16	2.06	0.05	2.84	0.07
Li	1.14	2.85	3.60	2.49	0.07	3.15	0.10
B	1.24	3.80	3.80	3.06	0.12		
C	1.33	3.82	3.82	2.87	0.23		
N	1.41	3.91	3.91	2.77	0.20		
O	1.51	3.87	3.87	2.57	0.13		
Ne	1.73	3.41	3.78	1.97	0.24	2.18	0.19

	RBE(10)			Relative Increase From Emtrance			
	Entrance	Bragg	Max	Bragg	σ	Max	σ
He	1.10	2.09	3.13	1.90	0.05	2.84	0.07
Li	1.13	3.12	3.64	2.75	0.07	3.21	0.12
B	1.22	3.70	3.72	3.04	0.10	3.06	0.24
C	1.30	3.84	3.84	2.96	0.20		
N	1.37	3.81	3.81	2.78	0.22		
O	1.45	3.82	3.82	2.64	0.13	2.64	0.13
Ne	1.65	3.37	3.73	2.04	0.24	2.26	0.19

Transverse RBE: 250 and 300mm depth beams



	RBE(10)			Relative Increase From Entrance			
	Entrance	Bragg	Max	Bragg	σ	Max	σ
He	1.09	1.74	2.92	1.59	0.04	2.67	0.06
Li	1.13	2.33	3.53	2.06	0.07	3.13	0.11
B	1.20	3.68	3.69	3.06	0.11	3.07	0.23
C	1.28	3.83	3.83	3.00	0.14		
N	1.34	3.84	3.84	2.87	0.17		
O	1.41	3.72	3.79	2.63	0.23	2.68	0.13
Ne	1.60	3.39	3.68	2.12	0.24	2.30	0.18

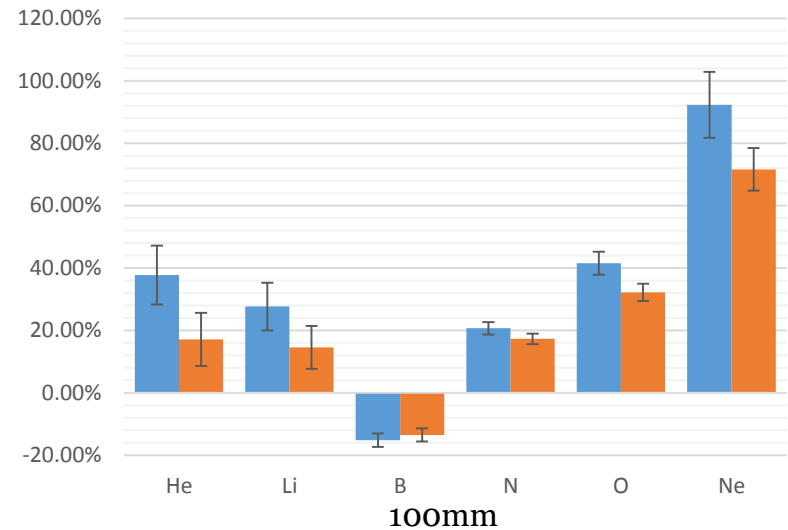
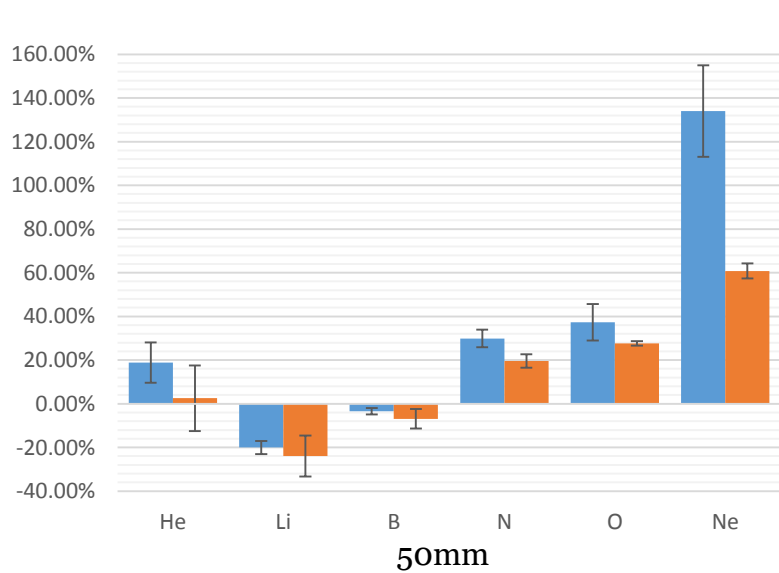
	RBE(10)			Relative Increase From Entrance			
	Entrance	Bragg	Max	Bragg	σ	Max	σ
He	1.09	2.01	2.72	1.83	0.17	2.49	0.17
Li	1.12	2.20	3.20	1.95	0.25	2.85	0.47
B	1.19	3.56	3.66	2.99	0.23	3.08	0.21
C	1.26	3.73	3.73	2.96	0.11		
N	1.32	3.79	3.79	2.87	0.18		
O	1.39	3.68	3.68	2.66	0.22	2.66	0.22
Ne	1.56	3.43	3.64	2.20	0.23	2.33	0.17

Transverse RBE: General Observations

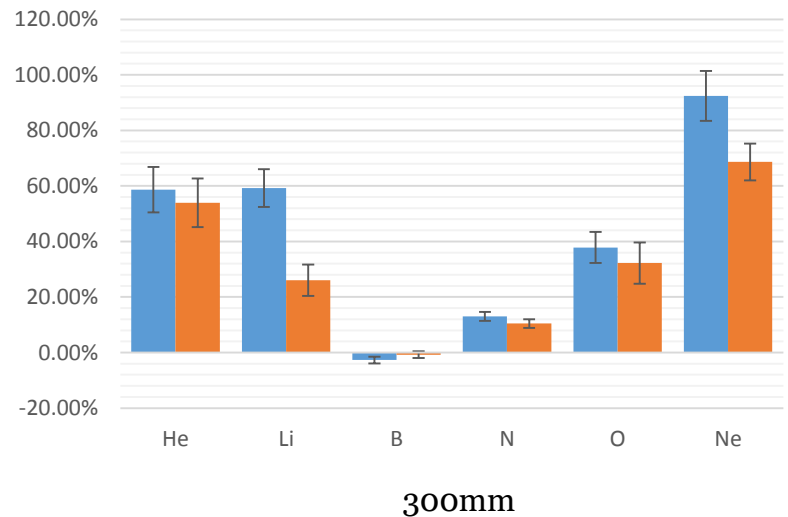
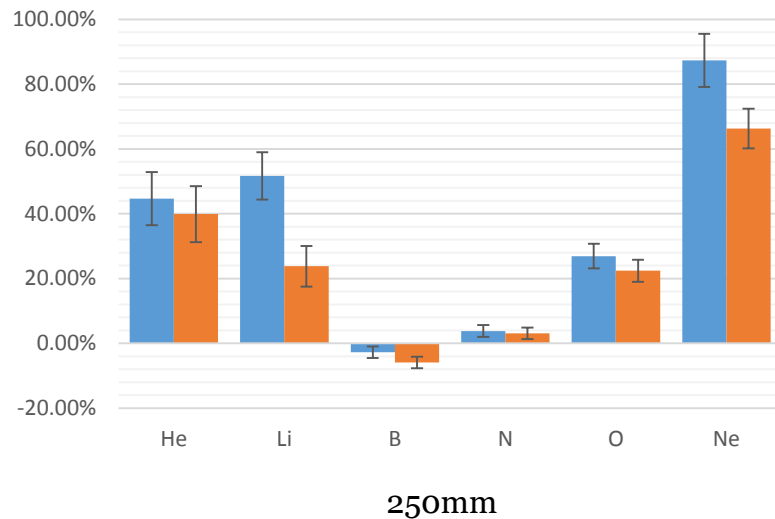
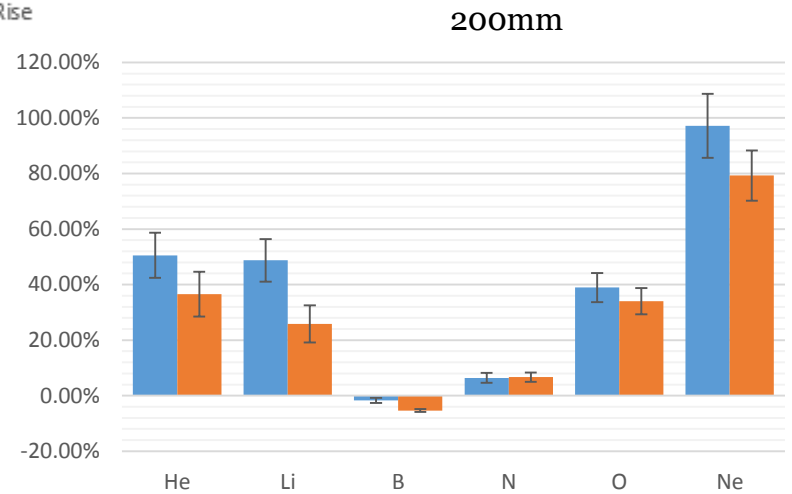
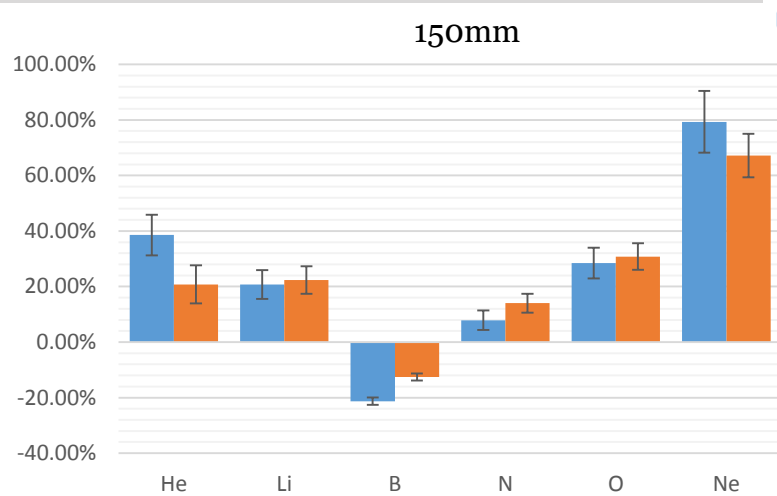
- For lighter ions (He, Li): Max RBE occurs distal to Bragg peak.
- Max RBE decreases as initial ion energy increases
- Boron shows greatest relative increase of initial RBE(10) to Bragg RBE(10)
 - Carbon shows similar increase especially as initial energy increases.
- From primary particles only, all ions heavier than He reach same approximate max RBE
 - Differences in max RBE of mixed field irradiations may be solely from different fragmentation yields of protons
 - Most apparent for lithium greater than 92MV/amu
- However, physical dose must be accounted for aswell...

Regional Biological Dose

- Regional Definitions:
 - Plateau: Phantom entrance until biological dose of “core” increases by 30%
 - Rise: From end of plateau, until “core” biological dose reaches 50% of max
 - Bragg: Region in which “core” biological dose is greater than 50% max
- Dose normalized to Bragg region dose, length, dose to ^{12}C regions



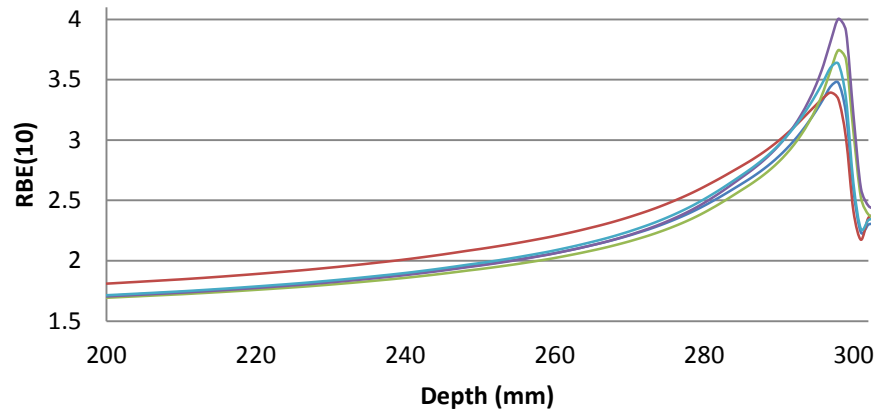
Regional Biological Dose: Relative to ^{12}C



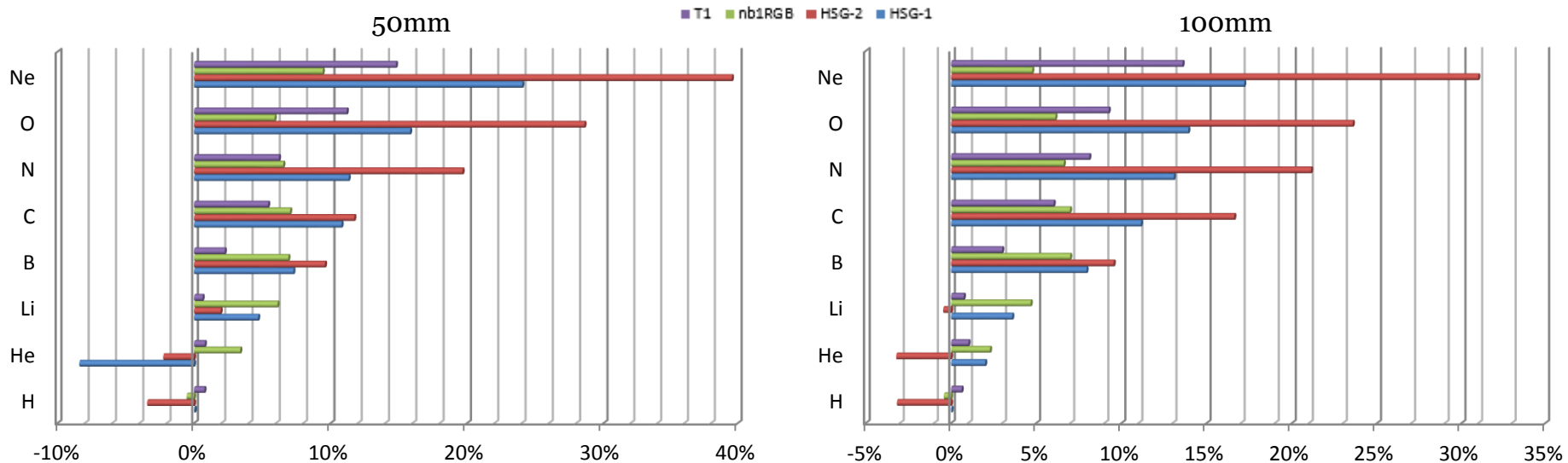
Regional Biological Dose: General Observations

- ${}^7\text{Li}$ highly favorable for low energy treatments, affected greatly by fragmentation at higher energies.
- Biological dose proximal to a lesion is reduced by the use of a ${}^{10}\text{B}$ beam. For the 100mm and 150mm beams this sparing is greatest, ~12-20% less than ${}^{12}\text{C}$.
- As initial energy increases ${}^{12}\text{C}$ and ${}^{14}\text{N}$ approach the sparing potential of ${}^{10}\text{B}$.
- Very simply comparison metric, but similar results to other metrics.
- In distal regions, low statistics make analysis difficult for RBE, but rule of thumb:
 - ${}^4\text{He}$, ${}^7\text{Li}$, ${}^{10}\text{B}$ and lower energy ${}^{12}\text{C}$ have similar dose fall offs (99% reduction within 1-3mm).
 - ${}^{14}\text{N}$, ${}^{16}\text{O}$, ${}^{20}\text{Ne}$ display much slower dose falloff (99% reduction within 10-50mm)

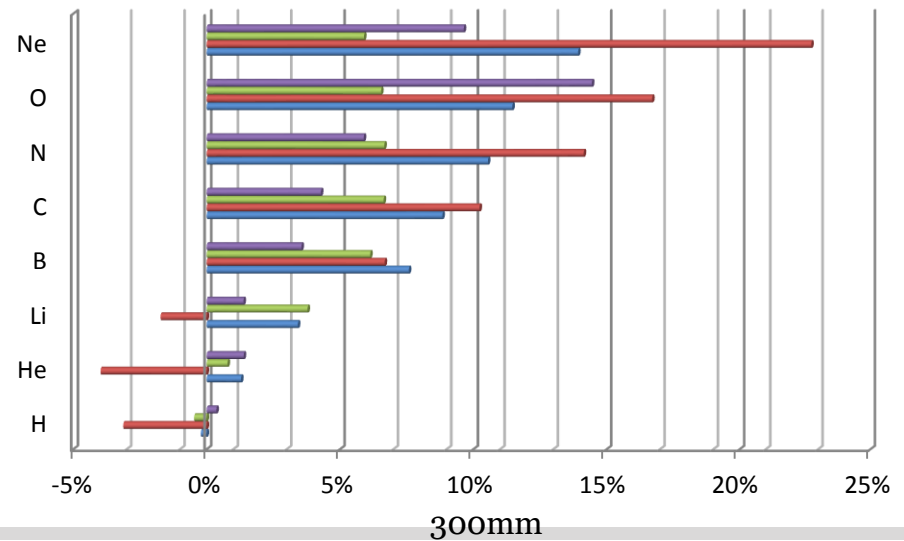
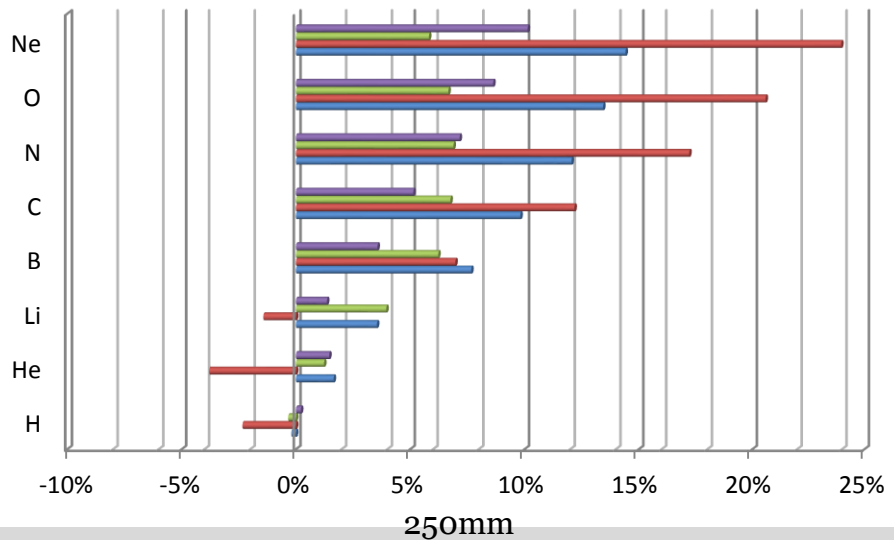
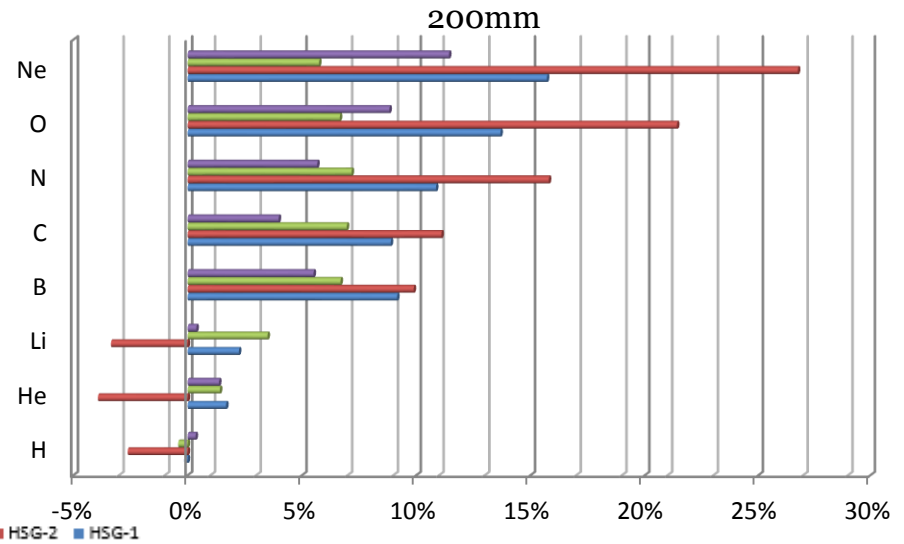
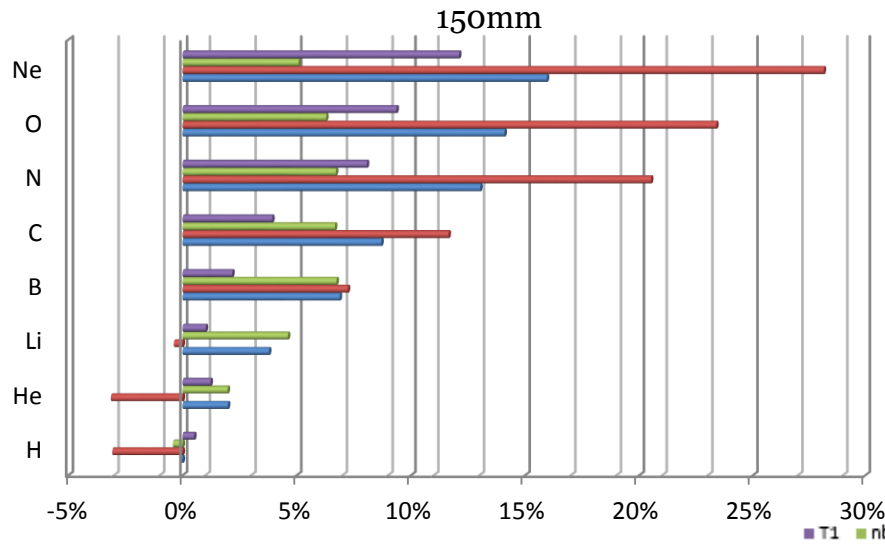
Cellular Dose: Compared to V79 Dose



- Cell specific doses normalized to regional doses of V79 cells
- Plateau region shown, rise region within $\pm 5\%$ of plateau ratios



Cellular Dose: Compared to V79 Dose



Cellular Doses: General Observations

- As particle charge increases, variance in cellular response increases
- As initial energy increases, variance in cellular response decreases
- V79 cells show greatest radiosensitivity for higher charged particles and in the regions of highest ionization density.
 - $\alpha/\beta=9.2$
- HSG cells show greatest radioresistance to protons and helium in areas of highest ionization density, but greatest radiosensitivity in areas of lower ionization density.
 - $\alpha/\beta=3.84, 5.09$
- Until Bragg region, ratio of cell specific RBE's remain relatively constant, could simplify planning calculations.

Conclusions

According to the MKM:

- Radial RBE variations exist, but have minimal effect on the dose-averaged RBE.
- ^{10}B may be a more appropriate ion than ^{12}C for ion therapy, especially for lesions 100-150mm in depth.
- According to conventional α/β ,
 - Early responding tumors may benefit most from ion therapy.
 - Proximal late responding tissues may be most negatively impacted.
 - Distal late responding tissues may be spared the greatest.
- This is just one model, in a very simplified setup. Lots of work still to be done.

Questions

References

Images

- Furusawa, Yoshiya. Radiation Quality and Biological Effects of Heavy Ion Beams. Radiological Sciences, Vol 50, No 7. (2007)
 - Zhang, R. et. Al. Predicted risks of radiogenic cardiac toxicity in two pediatric patients undergoing photon or proton radiotherapy. Rad. Onc. 8(184). (2013).
 - Furusawa, Y. (2014). Heavy-Ion Radiobiology in *Carbon Ion Radiotherapy*. Tokyo: Springer.
 - Inaniwa, T. et. al. Treatment planning for a scanned carbon beam with a modified microdosimetric kinetic model. Phys. Med. Biol. 55 (2010).
 - Particle and Heavy Ion Transport code System (PHITS). <https://phits.jaea.go.jp/Overview.html>
 - Sato T, Watanbe R, Nitta K. Development of a calculation method for estimating specific energy distribution in complex radiation fields. Radiation Protection Dosimetry. 2006; 122(41-45)
1. Wilson, RR. Radiological use of fast protons. Radiology. 47(5). 1946
 2. Particle Therapy Co-Operative Group (PTCOG): Patient Statistics (per end of 2015). https://www.ptcog.ch/archive/patient_statistics/Patientstatistics-updateDec2015.pdf
 3. U.S. Department of Energy. Workshop on ion beam therapy: summary report. (2013). https://science.energy.gov/~media/hep/pdf/accelerator-rd-stewardship/Workshop_on_Ion_Beam_Therapy_Report_Final_R1.pdf
 4. Chatterjee, A., Schaefer, H.J. Microdosimetric Structure of Heavy Ion Tracks in Tissue. Rad. And Environm. Biophysics 13: 215-227. 1976.
 5. Sato T, Niita K, Matsuda N, Hashimoto S, Iwamoto Y, Noda S, Ogawa T, Iwase H, Nakashima H, Fukahori T, Okumura K, Kai T, Chiba S, Furuta T, Sihver L. Particle and Heavy Ion Transport Code System PHITS, Version 2.62, J. Nucl. Sci. Technol. 50:9, 913-923 (2013).